Acta Cryst. (1977). B33, 527–537

γ-Brasses with *I* and *P* Cells

BY J. K. BRANDON, R. Y. BRIZARD, W. B. PEARSON AND D. J. N. TOZER

Physics Department, University of Waterloo, Waterloo, Ontario, Canada

(*Received* 26 *February* 1976; *accepted* 13 *July* 1976)

Single-crystal determinations of the structures of γ-brasses In_4Au_9 and In_4Ag_9 are reported. Both have primitive (*P*) cells and space group $P\bar{4}3m$. The structure of γ-Co–Zn was re-examined by X-ray powder photographs; no evidence was found for the *P* cell earlier reported. The ordering in Fe_4Zn_9 with the body-centred (*I*) cell is discussed. Factors that determine whether a cubic γ-brass adopts the *I*, *P* (or *F*) cell and that determine the ordering of the atoms therein are considered. These are: (i) obtaining a high value of the packing fraction, (ii) maximizing the number of contacts between unlike atoms and (iii) avoiding contact between the atoms present in lesser proportion, either because of their relative size, or for other reasons. Which of these effects dominates depends on the composition of the phase and the relative sizes of the component atoms. Calculation of the Ewald constant (α_{Ew}) for several phases with *I* cells, suggests that obtaining a high magnitude for it is also a factor in controlling the ordering of the atoms.

Introduction

Continuing our studies of γ-brasses, in this paper we report single-crystal determinations of the In_4Au_9 and In_4Ag_9 structures which Hellner & Laves (1947) recognized as having γ-brass-type structures. We have also carried out a powder diffraction examination of γ-Co–Zn, reported in Pearson (1958, 1967) to have a primitive (*P*) cell, but found to have the body-centred (*I*) cell.

In the main part of the paper we examine factors that determine whether a γ-brass adopts the *P* or *I* cell and that control the ordering therein. Generally these factors depend on the composition and relative sizes of the atoms insofar as they influence (i) the packing fraction, (ii) the number of contacts between unlike atoms, and, if composition permits it, (iii) the avoidance of close contacts between the larger atoms when the atoms differ by about 10% or more in size. When, however, the atoms are very disparate in size (more than 20 to 25%), achieving a high value of the packing fraction appears to be the main factor which controls the ordering.

The γ-brass structure can be described as built up of 26-atom clusters, composed of an inner tetrahedron (IT) of four atoms, followed by an outer tetrahedron (OT), an octahedron (OH) of six atoms and finally a cubo-octahedron (CO) of twelve atoms (Bradley & Jones, 1933). γ-Brasses with the *I* cell are composed of only one type of cluster packed as pseudoatoms in the b.c. cubic arrangement, those with the *P* cell of two clusters, *A* and *B*, packed as pseudoatoms in the CsCl structure arrangement, and those with the *F* cell (cell edge $2a_0$) of four clusters, *A*, *B*, *C* and *D*.

The structure of In_4Au_9

Single crystals were obtained from an alloy of composition In_4Au_9 prepared by melting 99·99% pure In and Au in an evacuated quartz tube followed by quenching in water. A spherical single crystal was spark-cut from the ingot and etched to remove surface strain and to reduce its size to approximately 0·04 mm radius. The remainder of the ingot was crushed and used for pycnometric density measurements which gave $D_m = 15{\cdot}60 \pm 0{\cdot}10$ g cm^{-3}.

Weissenberg and precession X-ray photographs indicated that the structure has Laue-symmetry class *m3m* and a primitive lattice, since there are no systematically absent reflexions. Possible cubic space groups are *P*432, No. 207; $P\bar{4}3m$, No. 215; and *Pm3m*, No. 223 (*International Tables for X-ray Crystallography*, 1969). $P\bar{4}3m$ was eventually chosen. An accurate value of the room-temperature cell constant, $a = 9{\cdot}829 \pm 0{\cdot}001$ Å, was determined by a least-squares fit to values of 2θ measured on a Syntex $P\bar{1}$ automatic four-circle diffractometer using graphite-monochromated Mo $K\alpha$ radiation ($\lambda = 0{\cdot}71069$ Å). The measured density and cell constants indicated $Z = 52$ atoms per unit cell for the stoichiometry In_4Au_9, since $D_x = 15{\cdot}61 \pm 0{\cdot}01$ g cm^{-3}.

Intensities were measured for 1484 reflexions over one eighth of reciprocal space with the same diffractometer and radiation, with an ω–2θ scan ($2° < 2\theta < 60°$). The scan rate was chosen to depend on the intensity of the reflexion being measured, 2° min^{-1} being usually selected since most reflexions were weak. The background was measured on both sides of each reflexion. The reflexion data were corrected for

background, Lorentz and polarization effects with the program *DATCO3* on the McMaster University computer. Program *AILOD* was used on the University of Waterloo IBM 360-75 computer to apply absorption corrections for a spherical crystal ($\mu = 1519$ cm^{-1} for Mo $K\alpha$ radiation, $\mu R = 5{\cdot}2$). The data were reduced by averaging symmetry-equivalent reflexions leaving 330 independent ones of which 324 were greater than zero. For all symmetry-equivalent reflexions the deviations of the intensities from their mean were less than 10%. Crystal data for In_4Au_9 are summarized in Table 1.

The starting model for structure refinement was that of Al_4Cu_9 (von Heidenstam, Johansson & Westman, 1968) in space group $P\bar{4}3m$, with In atoms replacing the Al atoms on *A* IT and *B* CO sites and Au atoms replacing Cu atoms elsewhere. Atomic scattering factors for In and Au for the Thomas–Fermi–Dirac statistical model, along with corrections for anomalous scattering with Mo $K\alpha$ radiation were taken from *International Tables for X-ray Crystallography* (1968). Least-squares refinements of this model with the

Table 1. *Crystal data for* In_4Au_9 *and* In_4Ag_9

	In_4Au_9	In_4Ag_9
Crystal system	Cubic	Cubic
Space group	$P\bar{4}3m$	$P\bar{4}3m$
Cell constant (Å)	9·829 ± 0·001	9·922 ± 0·004
Measured density, D_m (g cm^{-3})	15·60 ± 0·10	9·9 ± 0·4*
Atoms per unit cell, Z	52	52*
Calculated density, D_x (g cm^{-3})	15·61 ± 0·01	9·72
Absorption coefficient, (Mo $K\alpha$) (cm^{-1})	1519	262

* There was insufficient sample of this alloy available for accurate density measurements. Z was taken as 52 as for standard γ-brass structures.

Table 2. *Atomic coordinates and isotropic temperature factors for* In_4Au_9 *and* In_4Ag_9

Figures in parentheses are standard errors in the last digits quoted as derived in the least-squares refinement.

		In_4Au_9	($a_0 = 9{\cdot}829$ (1) Å)					In_4Ag_9	($a_0 = 9{\cdot}922$ (4) Å)			
Cluster	Site	Point set	Atoms	x	y	z	B (Å^2)	Point set	Atoms	x	z	B (Å^2)
A	IT	4(*e*) *xxx*	4 In	0·1212 (10)			0·7 (3)	4(*e*) *xxx*	4 In	0·122 (1)		1·5 (3)
B	IT	4(*e*) *xxx*	4 Au	0·6080 (6)			0·6 (1)	4(*e*) *xxx*	4 Ag	0·605 (1)		0·6 (2)
A	OT	4(*e*) *xxx*	4 Au	−0·1659 (8)			1·4 (2)	4(*e*) *xxx*	4 Ag	−0·162 (1)		0·6 (2)
B	OT	4(*e*) *xxx*	4 Au	0·3241 (7)			1·1 (2)	4(*e*) *xxx*	4 Ag	0·318 (1)		0·7 (2)
A	OH	6(*f*)00*z*	6 Au	0·0	0·0	0·3575 (10)	1·0 (1)	6(*f*)00*z*	6 Ag	0·0	0·355 (12)	1·8 (12)
B	OH	6(*g*)$\frac{1}{22}z$	6 Au	0·5	0·5	0·8566 (9)	0·9 (1)	6(*g*)$\frac{1}{22}z$	6 Ag	0·5	0·854 (12)	1·0 (9)
A	CO	24(*j*) *xyz*	9 Au + 3 In	0·3319 (9)	0·3031 (8)	0·0307 (7)	0·5 (1)	12(*i*) *xxz*	12 Ag	0·320 (1)	0·034 (2)	1·6 (2)
B	CO	24(*j*) *xyz*	9 In + 3 Au	0·8259 (9)	0·8000 (12)	0·5361 (9)	0·7 (2)	12(*i*) *xxz*	12 In	0·808 (1)	0·530 (2)	1·5 (2)

Table 3. *Interatomic distances in* Å *for* In_4Au_9

Estimated errors in distances are ±0·03 Å. For distances involving CO atoms, the x and y coordinates of Table 2 have been averaged to place the CO atoms on *xxz* sites (see text for discussion). A prime is used to indicate an atom in a neighbouring cluster whenever the *A* and *B* notation fails to make this distinction.

Number	Cluster *A*		Cluster *B*	
	A IT (In) to:		*B* IT (Au) to:	
3	*A* IT	3·37	*B* IT	3·00
3	*A* OT	2·89	*B* OT	2·95
3	*A* OH	2·87	*B* OH	2·87
3	*A* CO	2·86	*B* CO	2·93
1	*B* OT	3·46	*A* OT	3·85
	A OT (Au) to:		*B* OT (Au) to:	
3	*A* IT	2·89	*B* IT	2·95
3	*A* OH	2·98	*B* OH	3·02
3	*A* CO	2·86	*B* CO	2·82
3	*B* CO	2·94	*A* CO	2·89
1	*B* IT	3·85	*A* IT	3·46

Number	Cluster *A*		Cluster *B*	
	A OH (Au) to:		*B* OH (Au) to:	
2	*A* IT	2·87	*B* IT	2·87
2	*A* OT	2·98	*B* OT	3·02
1	*A* OH′	2·80	*B* OH′	2·82
4	*A* CO	3·16	*B* CO	3·13
2	*B* CO	2·80	*A* CO	2·77
2	*B* CO	3·14	*A* CO	3·06
	A CO ($\frac{3}{4}$ Au + $\frac{1}{4}$ In) to:		*B* CO ($\frac{3}{4}$ In + $\frac{1}{4}$ Au) to:	
1	*A* IT	2·87	*B* IT	2·93
1	*A* OT	2·86	*B* OT	2·82
1	*B* OT	2·89	*A* OT	2·94
2	*A* OH	3·16	*B* OH	3·13
1	*B* OH	2·77	*A* OH	2·80
1	*B* OH	3·06	*A* OH	3·14
2	*A* CO	3·99	*B* CO	3·85
2	*B* CO	2·93	*A* CO	2·88
2	*B* CO	2·88	*A* CO	2·93
2	*A* CO′	3·64	*B* CO′	3·75

program *LSTSQR* and unit weights converged to a relatively large R_1 value of about 0·20 ($R_1 \equiv \Sigma||F_o| - |F_c||/\Sigma|F_o|$). Numerous adjustments were made to the model along with the introduction of a weighting scheme and the refinement of an extinction correction parameter. This finally led to a structure in which there was some slight mixing of In with Au on *A* CO sites and some slight mixing of Au with In on *B* CO sites. The mixing of In and Au on CO sites did not improve the weighted R_w index $\{R_w \equiv [\Sigma w(|F_o| - |F_c|)^2/\Sigma wF_o^2]^{1/2}\}$ appreciably, but the mixing did yield more reasonable isotropic temperature factors for these sites. On the other hand R_w was quite sensitive to a new model in which each CO atom previously placed on a {110} mirror plane was shared between two related points slightly out of the mirror plane, a possibility pointed out earlier from construction of hard-sphere γ-brass models (Brandon, Brizard, Chieh, McMillan & Pearson, 1974). Such a model could be interpreted as representing either real random displacements of the CO atoms, or anisotropic thermal motion of CO atoms perpendicular to their mirror planes. The model using this 'split' CO atom description gave $R_w = 0{\cdot}082$ for the 324 reflexions with intensities greater than zero using the Cruickshank-type weighting scheme, $w = (17{\cdot}0\text{–}0{\cdot}040\ F_o + 0{\cdot}000025F_o^2)^{-1}$. The atomic coordinates and isotropic temperature factor parameters are given in Table 2, and the interatomic distances for In_4Au_9 are in Table 3 where the split CO atoms lying to either side of the mirror planes have had their coordinates averaged, corresponding to the time-average position under the interpretation of anisotropic thermal motion. Table 4 gives observed and calculated structure amplitudes based on the atomic parameters of Table 2. It is probable that R_w could not be reduced below 0·082 because many of the reflexions are quite weak, especially the class that arises from the *P* superstructure, and all 324 reflexions with intensities greater than zero have been included in this refinement.

Recent high-temperature powder work by Pušelj & Schubert (1975) using an alloy of composition $In_{31}Au_{69}$ and visual intensity estimation has shown a similar structure to that reported here, with R_1 based on *F* about 0·20. Their structure is of the Al_4Cu_9 type with no mixing of Au and In on either of the CO sites.

Table 4. *Observed and calculated structure factor amplitudes for* In_4Au_9

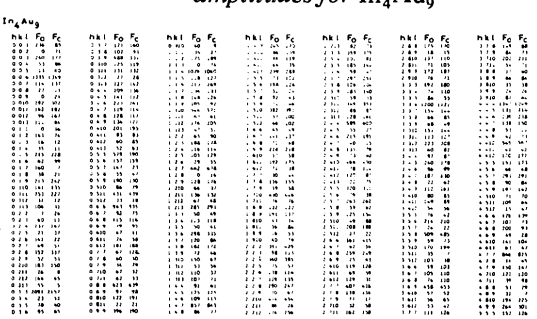

Crystal structure of In_4Ag_9

In retrospect the possibility of carrying out a conventional accurate structure refinement on In_4Ag_9 in space group $P\bar{4}3m$ appears remote because of the small number of observable reflexions with $h + k + l$ odd resulting from the small difference in atomic scattering factors of In and Ag with any radiation available to us. Nevertheless we have established without doubt that In_4Ag_9 has a primitive cubic cell rather than a b.c. cubic cell suggested by earlier work (Hellner & Laves, 1947; Hellner, 1951) and we have shown that the ordering is similar to that in Al_4Cu_9 with In in *A* IT and *B* CO. We do not, however, feel that the accuracy of the structure determination justifies full publication of atomic coordinates, interatomic distances and structure factors, although these are available from the authors on request. Instead, in Table 2, we show for comparison with In_4Au_9 'approximate' values of atomic coordinates resulting from refinement on data with $h + k + l$ even to $R_w = 0{\cdot}088$ (see below).

In the present work, an alloy of composition In_4Ag_9 was prepared in a quartz tube from 99·99% pure In and Ag, annealed at 270°C for 400 h and quenched in water. An irregular crystal about 0·1 mm diameter was selected from the crushed alloy. Weissenberg and precession X-ray photographs of the aligned crystal showed that the structure had Laue-symmetry class $m3m$, and the room-temperature cubic cell constant was measured for the single crystal mounted on a General Electric XRD-6 diffractometer by using a least-squares fit to six measured 2θ diffraction angles with no systematic corrections included. The crystal data are summarized in Table 1.

Intensity data were collected from the single crystal on the GE XRD-6 diffractometer with a scintillation counter and pulse-height analyser using Zr-filtered Mo $K\alpha$ radiation and the stationary-crystal stationary-counter method. 2284 reflexions were measured for a b.c. cubic lattice over half a hemisphere. The measured intensities were corrected for Lorentz and polarization effects with the program *DATAPREP* on the University of Waterloo IBM 360-75 computer. No correction was made for adjustment of intensity counts to integrated intensities as a function of 2θ. No absorption correction was applied, since $\mu R \simeq 1{\cdot}3$ with Mo $K\alpha$ radiation and a test indicated that one calculated on the basis of a spherical crystal approximation for the irregular sample would not be too satisfactory. Symmetry-equivalent reflexions were averaged and 230 observed reflexions remained of which 146 were con-

Table 5. *Observed 0kl reflexions with h + k + l odd*

003	014	047	056
005	016	0,4,11	069
007	0,1,10		078
0,0,11			

sidered observable above threshold. These reflexions were used for full-matrix least-squares refinement of the structure in $P\bar{4}3m$ on a model based on the ordering reported for Al_4Cu_9 (von Heidenstam, Johansson & Westman, 1968), placing In in *A* IT and *B* CO. The refined structure finally gave $R_w = 0{\cdot}088$ for the 146 observed reflexions using the Cruickshank-type weighting scheme $w = (215{\cdot}0 - 1{\cdot}0F_o + 0{\cdot}00188F_o^2)^{-1}$ and refining an extinction parameter. The refined coordinates give interatomic distances similar to those found for In_4Au_9 (Table 3) confirming the assignment of In to *A* IT in particular.

Evidence for the primitive cell comes from the observation of 12 very weak $h + k + l$ odd reflexions (Table 5) on an $0kl$ precession photograph. These include all of those $0kl$ types expected to be observed from the calculated value of the structure amplitudes, F_c, based on the above model, with the possible exception of 025 and 038. Since, however, the F_c values suggest that no more than about 10% of the weak reflexions with $h + k + l$ odd might be observable in diffractometer data, it was considered unprofitable to proceed further with the structure analysis by collecting a full data set.

The lattice type of the γ-Co–Zn unit cell

The report in Pearson (1958, 1967) that γ-Co–Zn had a *P* cell and our prediction that it should have an *I* cell, led to the preparation of a γ-Co–Zn alloy containing 80% Zn and its examination by powder X-ray diffraction. When this revealed no evidence for a *P* cell, the original papers by Ekman (1931) and Schramm (1938) were re-read with the discovery that the error lay with Pearson (1958, 1967) in mistakenly attributing this information to Schramm (1938). Earlier and present evidence all indicates that γ-Co–Zn has an *I* cell.

Discussion

Recently there has been revived theoretical interest in calculating phase stability in terms of first and second near-neighbour interactions (*cf.* for example Richards & Cahn, 1971; Allen & Cahn, 1972). The following discussion, taken with that in Booth, Brandon, Brizard, Chieh & Pearson (1977), shows that nearest neighbour interactions *M–M* (*M* is minor component) and *M–N* are important in determining whether γ-brasses adopt *I*, *P* or *F* cells and in determining the ordering of the atoms. The relative importance of these effects, however, depends on the relative sizes of the component atoms and when these are disparate, packing fraction considerations (Laves, 1956; Parthé, 1961) may dominate the scene. Calculations of an average Ewald constant suggest that maximizing the magnitude of this parameter is also a feature controlling the ordering in γ-brasses with *I* cells.

(*a*) *Minimizing the number of contacts, M–M, between the larger atoms*

One of the reasons for γ-brasses of composition M_4N_9 adopting the *P* cell is that this allows the larger *M* atoms to avoid the formation of *M–M* close contacts to a greater extent than can ordering schemes in the *I* cell. However, in *I*, *P* or *F* cells it is impossible to avoid some contacts between *M* atoms at this composition.

The *P* cell is built up of two different clusters, *A* and *B*, of 26 atoms, each of which has four sites, IT, OT, OH and CO. Following Booth *et al.* (1977), we assume that a large *M* atom on IT, OT, OH or CO sites will have the close neighbours shown in Table 6 where primes indicate contacts to atoms in neighbouring clusters. Thus, if *M* atoms are not to be close neighbours, they cannot be put on OH sites because of the OH–OH′ contacts that would ensue, or into IT sites because of the IT–IT contacts within the inner tetrahedron. If they are put in OT sites (say *B* OT), then the near neighbours of an *M* atom on an OT site are those shown by the numbers in Fig. 1(*a*). Since the OH sites are forbidden, *A* OT is the only other site where further *M* atoms can be added without making *M–M* close

Table 6. *Close neighbours*

(*a*)		(*b*)
IT–3 IT		
OT–3 IT	IT–3 OT	OT–3 CO′
OH–2 IT	IT–3 OH	OH–1 OH′
		2 CO′
CO–1 IT	IT–3 CO	CO–1 OT′
1 OT	OT–3 CO	1 OH′
		4 CO′

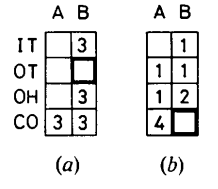

Fig. 1. Number of close neighbours of an atom on (*a*) an OT site and (*b*) a CO site provided by atoms on the sites indicated for a γ-brass with a *P* cell.

contacts. However, both *A* and *B* clusters would then be identical and the structure would reduce to the *I* type.

The *M* atoms must therefore be located in CO sites. If 12 *M* atoms are placed in *B* CO, say, Fig. 1(*b*) shows that no more *M* atoms can be introduced without making *M*–*M* close contacts. However, if four *M* are located in *A* IT the formula M_4N_9 is achieved and the only *M*–*M* contacts to occur are those *within* the *A* inner tetrahedron itself. This is indeed the basis of the ordering reported for Al_4Cu_9, γ_1-Ga_4Cu_9, In_4Ag_9 and In_4Au_9.

It can also be shown that there are two other effects which particularly influence the adoption of *P* or *I* cells and the ordering found therein.

(*b*) *Maximizing the number of unlike contacts, M–N*

γ-Brasses with *I* cells in which there are no vacant or partially vacant sites have been reported at composi-

Table 7. *γ Phases with the I cell*

M_xN_y*	*M* atom in sites†				Structures determined with ordering indicated, radius ratio, R_M/R_N, in parentheses	Weighted number of neighbours per cell			Packing fraction (PF) and Ewald constant ($-\alpha_{Ew}$) at ordering indicated							
x:*y*	IT	OT	OH	CO		*M–M*	*N–N*	*M–N*	Ni_2Zn_{11}		Ir_2Zn_{11}					
									P.F.		P.F.					
2:11	8					12	174	72	0·652		0·659					
		8			Ni_2Zn_{11}(0·894) Ir_2Zn_{11}(0·973)	0	174	84	0·642		0·665					
			8			$2\frac{2}{3}$	$188\frac{2}{3}$	$66\frac{2}{3}$	0·650		0·659					
				8		$5\frac{1}{3}$	$187\frac{1}{3}$	$65\frac{1}{3}$	0·628		0·658					
									Fe_3Zn_{10}		Pd_3Zn_{10}					
									PF	$-\alpha_{Ew}$	PF					
3:10	8	4				24	144	90	0·670	1·9376	0·660					
	8		4			$20\frac{2}{3}$	$146\frac{2}{3}$	$90\frac{2}{3}$	0·650	1·9330	0·658					
	4	8			Fe_3Zn_{10}(0·914)	15	141	102	0·660	1·9911	0·661					
		8	4		Pd_3Zn_{10}(0·987)	$4\frac{2}{3}$	$142\frac{2}{3}$	$110\frac{2}{3}$	0·659	1·9924‡	0·662					
			12			6	156	96	0·649	1·9762	0·659					
				12		12	156	90	0·625	1·7770	0·658					
									Fe_4Zn_9							
									PF	$-\alpha_{Ew}$						
4:9	8	8			Fe_4Zn_9(0·914)§	36	114	108	0·676	2·0718						
	8		8		Fe_4Zn_9(0·914)‖	$30\frac{2}{3}$	$120\frac{2}{3}$	$106\frac{2}{3}$	0·644	2·0223						
	8			8		$25\frac{1}{3}$	$111\frac{1}{3}$	$121\frac{1}{3}$	0·648	1·9719						
	4		12			21	123	114	0·642	2·0615						
	4			12		21	117	120	0·636	1·8666						
		8	8			$10\frac{2}{3}$	$112\frac{2}{3}$	$134\frac{2}{3}$	0·664	2·1000‡						
		4	12			12	120	126	0·662	2·0709						
			12	4		$17\frac{1}{3}$	$129\frac{1}{3}$	$111\frac{1}{3}$	0·649	1·9464						
			4	12		$22\frac{2}{3}$	$130\frac{2}{3}$	$104\frac{2}{3}$	0·643	1·7368						
				16		$21\frac{1}{3}$	$127\frac{1}{3}$	$109\frac{1}{3}$	0·616	1·8222						
									Cu_5Cd_8		V_5Al_8	Cu_5Zn_8		Ag_5Zn_8	Ag_5Cd_8	
									PF	$-\alpha_{Ew}$	PF	PF	$-\alpha_{Ew}$	PF	PF	
5:8	8	8	4		Cu_5Cd_8(0·815)#	$48\frac{2}{3}$	$90\frac{2}{3}$	$118\frac{2}{3}$	0·699	1·8604‡	0·676	0·686	1·8350	0·645	0·683	
	8		12			42	96	120	0·584	1·8474	0·649	0·640	1·8531	0·627	0·644	
	8			12		36	84	138	0·582	1·8082	0·650	0·647	1·8226	0·656	0·647	
	4	8	8		V_5Al_8(0·940)	$33\frac{2}{3}$	$87\frac{2}{3}$	$136\frac{2}{3}$	0·657	1·8331	0·675	0·674	1·8401	0·643	0·677	
		8	12		Cu_5Zn_8(0·917) Ag_5Zn_8(1·037) Ag_5Cd_8(0·922)	18	84	156	0·602	1·8280	0·672	0·662	1·8729‡	0·642	0·669	
		8		12		36	96	126	0·540	1·7688	0·632	0·615	1·8195	0·651	0·612	
6:7	8	8	8			$62\frac{2}{3}$	$68\frac{2}{3}$	$126\frac{2}{3}$								
	8	4	12			60	72	126								
	4	8	12			45	63	150								
	8		12	4		$57\frac{1}{3}$	$73\frac{1}{3}$	$127\frac{1}{3}$								
	4			20		$46\frac{2}{3}$	$66\frac{1}{3}$	$145\frac{1}{3}$								
		8	12	4		$37\frac{1}{3}$	$65\frac{1}{3}$	$155\frac{1}{3}$								
		4	12	8		$45\frac{1}{3}$	$77\frac{1}{3}$	$135\frac{1}{3}$								

* *M* is always the component present in the smaller proportion; thus in this table it is also generally the smaller atom.

† Although the orderings selected here are only those of apparent interest, the value of the maximum number of *M–N* contacts at each composition has been checked by computer program for all possible orderings assuming an average CN per atom of 11·77 for each site which is the average of the unweighted values used in the calculations here.

‡ Largest value obtainable.

§ This Fe_4Zn_9 model assumes the Fe atoms to be in IT and OT as found by Brandon *et al.* (1974) for a γ phase with lower Fe concentration at Fe_3Zn_{10}.

‖ This Fe_4Zn_9 model has the ordering of Johansson *et al.* (1968).

The structure reported by Brandon *et al.* (1974) for an alloy with slightly higher *M* concentration has essentially this ordering of *M* atoms.

tions centred on M_2N_{11}, M_3N_{10}, M_4N_9, M_5N_8 and M_6N_7. We have calculated the number of *M–M*, *N–N* and *M–N* contacts per unit cell for different plausible orderings at these compositions (Table 7) and the maximum number of *M–N* contacts obtainable is shown as a function of composition in Fig. 2.

The coordination polyhedra [as defined by Frank & Kasper (1958)] about atoms on IT, OT, OH and CO sites contain 12, 12, 13 and 15 atoms respectively. 34 of these neighbours (Table 6) form close contacts, generally at the radii sums or closer. Another 14 are at intermediate distances, and the remaining four are generally so far away that for present purposes they are not considered near neighbours. In counting the number of *M–M*, *N–N* and *M–N* neighbours, the 34 close contacts are given full weight and the 14 intermediate contacts are given half weight, since in 15 γ-brass structures with *I*, *P* or *F* cells that have been determined (ignoring those with vacant sites and the close Sn–Cu contacts in $Sn_{11}Cu_{41}$ and Sn_3Cu_9Ni), the average difference between these observed distances and those calculated as the CN 12 radii sums is 0·143 Å. This average increase in bond length corresponds reasonably closely to the value 0·18 Å calculated from Pauling's (1947) bond order equation, $R_{(1)} - R_{(n)} = 0{\cdot}30 \log n$ for the increase in radius when the bond decreases to half its strength.

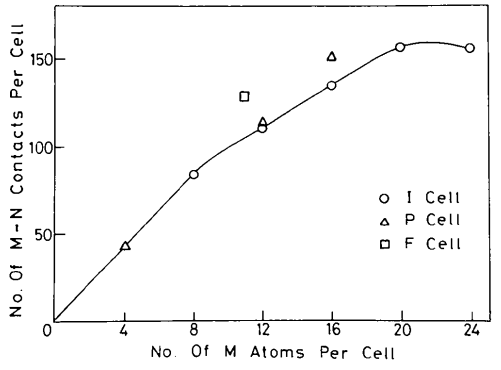

Fig. 2. Maximum number of *M–N* close contacts (weighted: see text) obtainable in γ-brasses M_xN_y ($x < y$) with *I* cells (○) as a function of the number of *M* atoms per cell. △ indicates the number obtained in *P* cells with 4 *M* in OT, 12 *M* in CO and 16 *M* in *A* IT and *B* CO. □ indicates one eighth of the number obtained in the *F* cell of $Sn_{11}Cu_{41}$ (Booth *et al.*, 1977).

Similar calculations based on the observed ordering for the *P* cell at a composition M_4N_9 and for the *F* cell $M_{11}N_{41}$ (giving full weight to all close Sn–Cu contacts) show a notable increase in the number of unlike *M–N* contacts (Table 8), compared to the maximum number obtainable in the *I* cell (Fig. 2 and Table 7). This would appear to be a further reason for structures adopting *P* or *F* cells at these compositions. It can also be noted from Fig. 2 that there is little increase compared to the *I* cell in the maximum number of *M–N* contacts for the *P* cell at a composition M_3N_{10} with the obvious ordering putting 12 *M* into one of the CO positions (*i.e.* giving no *M–M* contacts, Table 8). This is perhaps a contributing reason for no *P* cell being reported at this composition.

It is interesting to note that the weighted numbers of *M–N* neighbours obtained per atom by putting one component (*M*) alone into IT, OT, OH or CO sites in the *I* cell are in the ratio 18:21:16:11 respectively. Thus OT is the most effective site for creating *M–N* neighbours, and it is occupied by the component present in lesser proportion in all structures so far determined to have *I* cells, with the possible exception of Fe_4Zn_9 whose reported ordering (Johansson, Ljung & Westman, 1968) is in dispute (see below). This can be interpreted as further evidence that the creation of unlike neighbours is an important feature in the ordering of γ-brasses with *I* cells.

As a final check that the figures given in Table 7 for the maximum number of *M–N* contacts are indeed the maximum numbers or very close to them, we have written a computer program to calculate the number of *M–N* contacts for each of the compositions M_xN_y, assuming an average CN of 11·77 per site and varying the ordering in steps of two atoms. The results obtained by inspection and manual calculations (Table 7) are indeed confirmed.

Table 8. *Ordering of M atoms and weighted number of neighbours per cell for M_xN_y structures with F or P cells*

x:*y*	Cell	Ordering of *M* atoms	Weighted number of neighbours per cell* *M–M*	*N–N*	*M–N*	Structures determined with ordering indicated, radius ratio, R_M/R_N, in parentheses
11:41	*F*	*A* OT:16; *B* CO:48; *D* OH:24	0	153	129†	$Sn_{11}Cu_{41}$ (1·209) Sn_3Cu_9Ni
3:10	*P*	*B* CO:12	0	144	114	
4:9	*P*	*A* IT:4; *B* CO:12	6	102	150	Al_4Cu_9 (1·121); γ_1 Ga_4Cu_9 (1·104); In_4Ag_9 (1·151); In_4Au_9 (1·153)

* Divided by 8 for the *F* cell.
† Giving full weight to all Cu–Sn close contacts.

After the next section dealing with packing fractions, we make further observations on the number of M–N contacts occurring in I phases at the ordering reported in structure determinations.

(c) *Maximizing the packing fraction*

The nature of the 26-atom clusters in γ-brasses and the way that they can be built up by assembling successively the inner and outer tetrahedra, followed by the octahedron and then the cubo-octahedron, suggest that the hard-sphere model can reasonably be used to construct and pack the clusters together to determine the minimum cell edge or best packing fraction (Laves, 1956; Parthé, 1961) as a function of the relative radii of the atoms on the four site sets in the I cell.

Assuming then the atoms to be hard spheres, the inner tetrahedron is first constructed with each IT atom in contact with three other IT atoms. Four OT atoms placed about IT each make contact with three IT atoms, the six OH atoms next located each make contact with two IT atoms provided that the radii are not very dissimilar, and the 12 CO atoms finally located normally make contact with one IT and one OT atom. Thus the compulsory contacts formed are those listed in Table 6(a). When the clusters are packed together, the compulsory contacts normally occurring between the clusters are those listed in Table 6(b), where a prime indicates an atom in a neighbouring cluster.

We have calculated the best packing fraction [$\varphi = 4\pi(xR_M^3 + yR_N^3)/3a^3$, where $x + y = 52$] with relative radii varying from 0·80 to 1·20 for atoms on the four sites in the I cell. We select values for the relative radii of atoms on the IT, OT and OH sites and the value of the relative radius of the atoms on CO sites is obtained by normalization of the total volume of the spheres in the unit cell to the value $208\pi/3$, obtained when the relative radii are 1·0 for the atoms on all four sites. Having selected the relative radii of the atoms for any case being calculated, the inner tetrahedron is assembled followed by the outer tetrahedron and octahedron. This establishes the locus of possible positions of atoms on the CO sites. The clusters are now packed together with adjustment of the positions of the CO atoms along their loci so as to obtain the minimum cell edge or maximum packing fraction. Thus we have calculated the maximum value of the packing fraction in a three-dimensional parameter space representing the relative normalized radii of the atoms in IT, OT and OH sites in steps of 0·04 from 0·80 to 1·20. Fig. 3 shows typical packing-fraction contours as a function of R_{OT} and R_{OH} for a section at $R_{IT} = 1{\cdot}00$. The largest values of the packing fraction are found in a narrow column through the three-dimensional parameter space as indicated in Fig. 4. The 26-atom clusters in γ-brass with the I cell pack together as pseudoatoms in the b.c. cubic arrangement and it is interesting to note that the highest packing fraction obtainable for a γ-brass (71%) exceeds that for the b.c. cubic structure (68%). This is because the 26-atom clusters give rise to good tetrahedral configurations of the atoms.

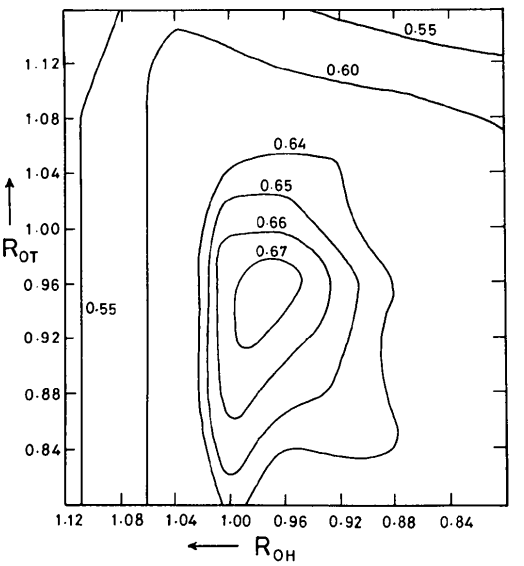

Fig. 3. Typical packing fraction contours for a γ-brass with the I cell, as a function of normalized relative radii R_{OT} and R_{OH}, in section at $R_{IT} = 1{\cdot}00$.

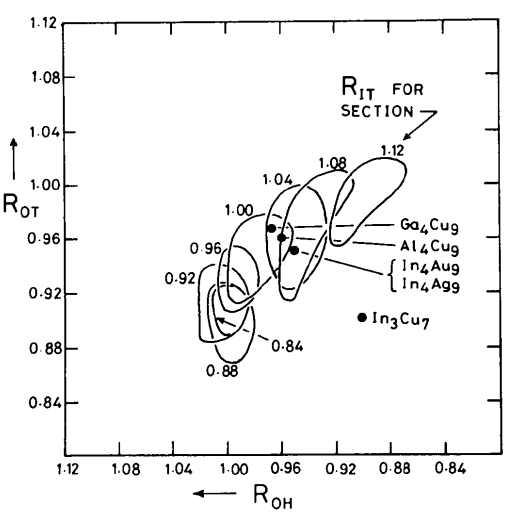

Fig. 4. Contours showing the highest packing fraction obtained in γ-brasses with I cells as a function of normalized relative radii, R_{OT} and R_{OH}, for sections with the R_{IT} values indicated. The contours have the following values of the packing fraction expressed as percentages: for $R_{IT} = 0{\cdot}84$ and 0·88, 70%; 0·92, 69%; 0·96, 68%; 1·00, 67% and for $R_{IT} = 1{\cdot}04$, 1·08 and 1·12, 66%. ● indicates the R_{OT} and R_{OH} values for the four phases named which have the P cell, and for In_3Cu_7 if Cu atoms occupy OT and OH sites in the A and B clusters.

(d) Assessment of the influence of the number of unlike contacts and the value of the packing fraction on the structure and ordering of γ-brasses

Table 7 gives data for ten γ-brasses with the *I* cell whose structures have been determined (excluding γ_3-Ag–Li which is not understood). The table lists the ordering reported for these structures, the radius ratio, the number of *M–N* contacts, the packing fraction calculated for that ordering and radius ratio, and the calculated value of the Ewald constant (see below). It also compares these values with the number of *M–N* contacts, the value of the packing fraction and the value of the Ewald constant obtained for these phases with other plausible orderings of the atoms. For models with mixed occupancies on any site, packing fractions have been calculated with radii values weighted in the proportion of the mixture. It can be seen that the phases with *I* cells generally order so as to form the largest possible number of *M–N* contacts consistent with also obtaining high (even if not the highest possible) values of the packing fraction and Ewald constant. The one exception to this is the Cu_5Cd_8 phase whose ordering does not maximize the number of Cu–Cd contacts nor minimize the number of Cd–Cd contacts between the large atoms, but gives the highest value of the packing fraction relative to other plausible orderings. In this case the relative sizes of the atoms are very disparate and the packing fraction, which is very sensitive to the type of ordering adopted, dominates other effects and controls the ordering.

Table 8 gives the ordering and the number of interatomic contacts for $Sn_{11}Cu_{41}$ and Sn_3Cu_9Ni with the *F* cell, and for four phases with the *P* cell. Although it is too complicated to determine the packing fraction for structures with the *P* cell, it can be seen from the positions (R_{OT} and R_{OH} values) of Al_4Cu_9, γ_1-Ga_4Cu_9, In_4Ag_9 and In_4Au_9 in Fig. 4, that they must have very high packing fractions since their R_{IT} values must lie between 1·00 and 1·04. Hence the *P* cell of these compounds is favoured not only by minimizing the number of *M–M* contacts between the large atoms and by maximizing the number of unlike *M–N* contacts, but also by achieving a high value of the packing fraction. The *F* cell of $Sn_{11}Cu_{41}$ and Sn_3Cu_9Ni avoids the formation of contacts between the large Sn atoms, and gives a larger number of unlike contacts *M–N* than could be obtained in an *I* cell.

(e) Electrostatic energies of γ-brass models

We have also attempted calculations of the Ewald electrostatic potential energy of positively charged metal point ions embedded in a uniform compensating background of negative charge for a few γ-brass structures with an *I* cell under a variety of ordering schemes. The method of calculating the Ewald energy per ion, U_E, has been discussed for simple metallic structures (Heine & Weaire, 1970; Sholl, 1967; Fuchs, 1935), and takes the form

$$U_E = \alpha_{Ew}\frac{z^2}{2R_a} \qquad (1)$$

where z is the effective valence and R_a is the radius of a sphere with the same volume per atom as the structure. The quantities in equation (1) are in atomic units. U_E is determined, apart from scaling constants, by the dimensionless parameter α_{Ew}, called the Ewald constant, which contains all the structurally dependent information.

For more complicated arrangements of metallic ions (more than one type of site), the Ewald energy can be cast into the same form containing an Ewald constant as its structurally dependent part which is now a tensor of second rank and containing the effective valences as components of a vector. For *I* cell γ-brasses we have the following equation

$$U_E = \frac{1}{2an}(z_1,z_2,z_2,z_4)\begin{pmatrix}\alpha_{11} & \alpha_{12} & \alpha_{13} & \alpha_{14}\\ \alpha_{21} & \alpha_{22} & \alpha_{23} & \alpha_{24}\\ \alpha_{31} & \alpha_{32} & \alpha_{33} & \alpha_{34}\\ \alpha_{41} & \alpha_{42} & \alpha_{43} & \alpha_{44}\end{pmatrix}\begin{pmatrix}z_1\\ z_2\\ z_3\\ z_4\end{pmatrix} \qquad (2)$$

where n is the number of atoms in the unit cell. The indices 1, 2, 3 and 4 refer to the IT, OT, OH and CO site-sets respectively of γ-brass and a is the cell edge. The tensor is symmetric ($\alpha_{ij} = \alpha_{ji}$) (Brizard, 1975).

Values of this Ewald tensor for three γ-brass phases, Cu_5Zn_8, Cu_5Cd_8 and Fe_3Zn_{10}, calculated using the atomic coordinates quoted by Brandon *et al.* (1974) appear in Table 9. It is noticeable in Table 9 that there is a variation in the Ewald tensor $\overleftrightarrow{\alpha}$ from one γ-brass to another due to the variation in atomic coordinates. There is also a large range of values for the individual elements of the tensor for a given structure. This indicates that permutation of valence inside the vector will change U_E appreciably; in short that ordering might be important.

Table 9. *Ewald-constant tensors for some γ-brass phases*

Cu_5Zn_8

$$-\begin{pmatrix}29{\cdot}0046 & 0{\cdot}0916 & 12{\cdot}4151 & 40{\cdot}9457\\ & 44{\cdot}7345 & 13{\cdot}5421 & 24{\cdot}5524\\ & & 73{\cdot}6828 & 29{\cdot}7174\\ & & & 168{\cdot}220\end{pmatrix}$$

Cu_5Cd_8

$$-\begin{pmatrix}19{\cdot}0512 & -5{\cdot}0865 & 11{\cdot}8157 & 39{\cdot}0632\\ & 43{\cdot}7491 & 12{\cdot}5221 & 24{\cdot}1353\\ & & 74{\cdot}4325 & 33{\cdot}2068\\ & & & 176{\cdot}059\end{pmatrix}$$

Fe_3Zn_{10}

$$-\begin{pmatrix}25{\cdot}3868 & -1{\cdot}8030 & 12{\cdot}1008 & 39{\cdot}4850\\ & 44{\cdot}3942 & 13{\cdot}1024 & 23{\cdot}8186\\ & & 74{\cdot}0510 & 31{\cdot}7793\\ & & & 173{\cdot}078\end{pmatrix}$$

Let us study the ordering for the hypothetical case where the atomic coordinates are independent of the ordering. For this study we want to keep the composition fixed and, therefore, the number of free electrons per unit cell fixed. The last condition is expressed mathematically by the next identity

$$n\bar{z} \equiv n_1 z_1 + n_2 z_2 + n_3 z_3 + n_4 z_4 \qquad (3)$$

where z is the average valency per atom and is the quantity kept constant to study ordering; n_1, n_2, n_3 and n_4 are the number of IT, OT, OH and CO atoms in the unit cell. We will also use the identity

$$R_a = \left(\frac{3}{4\pi n}\right)^{1/3} a \qquad (4)$$

for cubic crystals, to bring equation (2) in perfect correspondence with equation (1). Substituting a in terms of R_a from (4) into equation (2) and introducing $\bar{z}$ into the same equation, we obtain

$$U_E = \frac{1}{n}\left(\frac{3}{4\pi n}\right)^{\frac{1}{3}} \frac{\mathbf{z}}{\bar{z}} \leftrightarrow \alpha \frac{\mathbf{z}}{\bar{z}} \quad \frac{\bar{z}^2}{2R_a}. \qquad (5)$$

We have between equations (1) and (5) the correspondence

$$\alpha_{\mathrm{Ew}} = \frac{1}{n}\left(\frac{3}{4\pi n}\right)^{\frac{1}{3}} \frac{\mathbf{z}}{\bar{z}} \leftrightarrow \alpha \frac{\mathbf{z}}{\bar{z}}. \qquad (6)$$

The vector $\mathbf{z}/\bar{z}$ has its components in units of average valency and, using relation (3), we can express one of the components in terms of the other three; here our choice is the elimination of $z_4/\bar{z}$ as an independent variable

$$\frac{z_4}{\bar{z}} = \frac{n - (n_1 z_1/\bar{z} + n_2 z_2/\bar{z} + n_3 z_3/\bar{z})}{n_4}. \qquad (7)$$

In Table 10 we give a few values of α_{Ew} for γ-brasses and some simple structures having a cubic cell. For the values of z we use the Hume–Rothery convention for the valency and neglect the depletion hole correction (Heine & Weaire, 1970).

Table 10. *Values of* α_{Ew} *for some cubic structures*

Structure	$\mathbf{z}/\bar{z}$	$-\alpha_{\mathrm{Ew}}$
γ-Brass Fe_3Zn_{10}	(13/20, 0, 13/10, ···)*	1·9911
γ-Brass Cu_5Zn_8	(26/21, 13/21, 13/21, ···)*	1·8729
γ-Brass Cu_5Cd_8	(52/83, 52/83, 91/83, ···)*	1·8537
B.c.c. (disordered β-brass)	(1)	1·79186†
F.c. cubic	(1)	1·79175†
γ-Brass Cu_5Zn_8	(1, 1, 1, . . .)‡	1·7840
γ-Brass Fe_3Zn_{10}	(1, 1, 1, . . .)‡	1·7703
Simple cubic	(1)	1·76012†
γ-Brass Cu_5Cd_8	(1, 1, 1, . . .)‡	1·7407

* This uses the site occupancy as given in Brandon *et al.* (1974).
† Values from Heine & Weaire (1970, p. 271).
‡ Same charge on every ion.

The Ewald constant can be considered as a measure of the perfection of an arrangement of $1/r$ potentials; the first three entries in Table 10 are for an arrangement of potentials with different strengths whereas the rest are for potentials of the same strength. A comparison between the values obtained for the γ-brasses with $\mathbf{z}/\bar{z} = (1,1,1,1)$ and the tetrahedral error parameter calculated by Brandon, Chieh, Pearson & Riley (1975) for the same γ-brasses is interesting. Before doing the above calculations we expected a large value of $|\alpha_{\mathrm{Ew}}|$ to correlate with a small value of the error parameter, since the tetrahedral error parameter is a measure of the perfection of a tetrahedral arrangement and a regular arrangement should minimize the repulsion between the potentials, but this is not apparent. The error parameter values for Cu_5Zn_8, Cu_5Cd_8 and Fe_3Zn_{10} are respectively 7·70, 6·50 and 6·74%.

Values of α_{Ew} have also been calculated for γ-brass phases Fe_3Zn_{10}, Fe_4Zn_9, Cu_5Zn_8 and Cu_5Cd_8 for all possible orderings in steps of two atoms in each of the four site sets. The independent variables for the I cell are the numbers m_1, m_2 and m_3 of atoms of the less numerous kind (M) in the alloy formula, in site sets IT, OT and OH. We have the following relation between m_i and $z_i/\bar{z}$ supposing a formula $M_xN_{(1-x)}$ for the alloy:

$$\frac{z_i}{\bar{z}} = \frac{[m_i z_M + (n_i - m_i) z_N]}{n_i [x z_M + (1-x) z_N]}; \; i = 1, 2 \text{ and } 3. \qquad (8)$$

The values of α_{Ew} obtained for the plausible orderings listed in Table 7 are included in that table. The largest magnitudes of α_{Ew} obtainable for any possible ordering are indeed those obtained at the observed ordering in Cu_5Zn_8 and Cu_5Cd_8. For the observed ordering in Fe_3Zn_{10}, the magnitude of α_{Ew} is the second highest obtained, being only slightly less than that found for another ordering. For Fe_4Zn_9 the magnitude of α_{Ew} obtained for the ordering proposed in the next section is the largest obtainable with any possible ordering. Hence it appears that maximizing the magnitude of the Ewald constant is also an important factor in controlling the ordering and atomic positions in γ-brasses. This is particularly striking in the case of Cu_5Cd_8 where the ordering adopted neither minimizes the number of contacts between the larger Cd atoms, nor maximizes the number of unlike Cu–Cd contacts, but maximizes the packing fraction and the magnitude of the Ewald constant.

(*f*) *Ordering in* Fe_4Zn_9

Johansson, Ljung & Westman (1968), who determined the structure of γ-Fe_4Zn_9 with the I cell by single-crystal methods, placed eight Fe in IT and eight Fe together with four Zn in OH. Our single-crystal determination of the structure of Fe_3Zn_{10} (Brandon *et*

al., 1974) located four Fe + four Zn in IT and eight Fe in OT and would, therefore, require Fe_4Zn_9 to have eight Fe in IT and eight Fe in OT, since both compositions lie in a homogeneous phase field.

Johansson *et al.* (1968) studied the structure of Fe_4Zn_9 both by X-ray single-crystal methods (giving $R_1 = 0{\cdot}11$) and by powder neutron diffraction methods. Using their X-ray structure factors and our ordering of eight Fe in each of IT and OT, we obtain $R_1 = 0{\cdot}12$, whereas using their structure factors and their ordering of eight Fe in IT and eight Fe in OH we achieve the same refinement as Johansson *et al.* with $R_1 = 0{\cdot}11$. On the other hand, the data given in Table 7 suggest that neither of these orderings is correct. A significantly greater number of unlike *M–N* contacts (in fact the greatest number) can be obtained by placing eight Fe in OT and eight Fe + four Zn in OH, and this ordering also gives the largest magnitude of the Ewald constant. A refinement of the structure based on this ordering and using the X-ray structure factors of Johansson *et al.* gave an R_1 value (0·12) similar to those of the other orderings discussed above. Thus structural refinement based on existing structure factors gives little guidance to which is the correct ordering, although indirect evidence summarized below favours the ordering with Fe in OT and OH (referred to as BBP&T) over that with Fe in IT and OT (referred to as BBCM&P). Least favoured is that with Fe in IT and OH (referred to as JL&W).

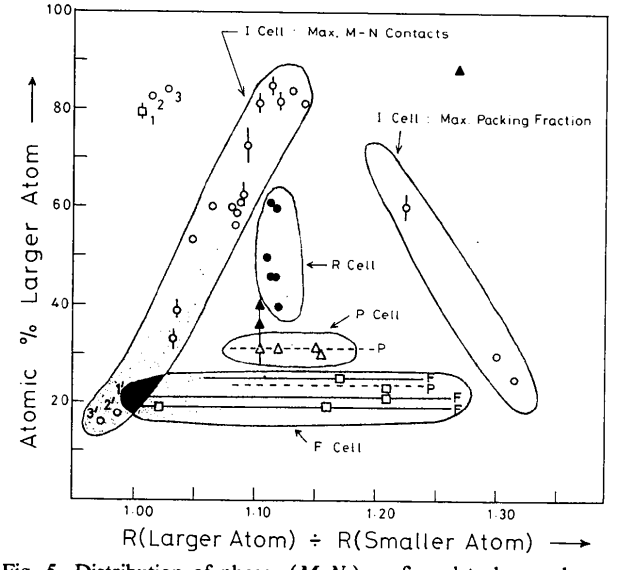

Fig. 5. Distribution of phases (M_xN_y) confirmed to have γ-brass type structures with *I* (○), *P* (△), *F* (□) or *R* (●) cells on a diagram of at.% *M* (the larger atom) *versus* the radius ratio, R_M/R_N. The Pt–Zn, Pd–Zn and Ir–Zn phases (1,2,3) with radius ratios close to unity are also included at 1′, 2′ and 3′ with *M* and *N* reversed. ▲ indicates phases with *P* cells and half or more of one of the IT site-sets vacant. The γ-Ag–Li phases are omitted from the diagram. Each horizontal broken line represents positions in the plot where ordering in *P* cells might be expected when $1{\cdot}10 \lesssim R_M/R_N \lesssim 1{\cdot}25$. These broken lines occur at compositions corresponding to formulae M_4N_9 and M_3N_{10} which allow plausible ordering schemes (Table 8). Each horizontal full line represents positions in the plot where ordering in *F* cells might be expected. These full lines occur at compositions MN_3 [see discussion of γ-$Sn_2Al_2Cu_{12}$ in Booth *et al.* (1977)], $M_{11}N_{41}$ and M_5N_{21}.

(1) All other γ-brass structures with *I* cells so far determined have atoms of the minor component in the OT site.

(2) Packing fractions are 0·676 (BBCM&P), 0·664 (BBP&T) and 0·644 (JL&W).

(3) Weighted numbers of unlike neighbours *M–N* per cell are ~135 (BBP & T), ~108 (BBCM & P) and ~107 (JL&W).

(4) Values of the Ewald constant (α_{Ew}) are:

	(BBP&T)	(BBCM&P)	(JL&W)
For atomic coordinates given by (JL&W):		−2·0766	−2·0346
For atomic coordinates adopted from (BBCM&P):	−2·1000	−2·0718	−2·0223

(5) Of the interatomic distances reported by (JL&W), OT–CO = 2·614 Å and OT–CO′ = 2·598 Å better satisfy Fe–Zn contacts (BBP&T, BBCM&P) than Zn–Zn contacts (JL&W). OT–IT = 2·492 Å better satisfies Fe–Fe contacts (BBCM&P) than Fe–Zn (JL&W, BBP&T), although OH–OH′ = 2·603 Å better satisfies mixed Fe–Zn contacts (JL&W, BBP&T) than Zn–Zn contacts (BBCM&P).

(*g*) *Summary of conditions controlling ordering in cubic γ-brasses*

γ-Brasses are formed between a Group II, III or IV metal and a transition, noble, rare-earth or thoride metal.

The composition of γ-brasses with cubic structures is controlled by electron concentration. 88 to 89 e per 52-atom cell is the highest *e/a* ratio normally obtained, although there is some indication (Brandon, Pearson, Riley, Chieh & Stokhuyzen, 1977) that phases with *R* cells are stable at considerably higher electron concentrations.

We now see that the type of cubic cell that a γ-brass, M_xN_y, adopts and the ordering of the atoms therein is generally controlled by three factors: (i) obtaining a high value of the packing fraction, (ii) maximizing the number of contacts between unlike atoms, (iii) avoidance of contact between the minor component atoms (*M* in M_xN_y) when $1{\cdot}10 \lesssim R_M/R_N \lesssim 1{\cdot}25$ and $x/y < 4/9$, or for reasons other than relative size. Theoretical calculations indicate that the ordering in three γ-brass phases with *I* cells which were considered is such as to maximize the magnitude of the Ewald constant – *i.e.* the structurally dependent component of the Ewald energy. Which of the factors (i) to (iii) is dominant depends

both on the composition and the relative sizes of the atoms. When the atoms are moderately disparate in size and there is less than ~25% of the larger atoms, ordering in *P* or *F* cells occurs to minimize contacts between the larger atoms, but when the phase contains a higher proportion of the large atoms and many contacts must occur between them, the *I* cell results. When the atom sizes are very disparate, the packing fraction is very sensitive to the type of order and it is the dominant effect controlling the ordering in the *I* cell.

Thus we expect γ-In_3Cu_7 and γ-$InMn_3$ with γ-brass structures and radius ratios 1·30 and 1·315 not to order in the *P* cell with In in *A* IT and *B* CO (Fig. 4 suggests that such ordering for In_3Cu_7 would give a very poor value of the packing fraction), but to order with 4 In in OH and 12 and 9 respectively in CO (probably in the *I* cell) so as to give very high packing fractions of about 0·7 in each case. High-temperature powder photographs of γ-In–Cu indicate that the phase has an *I* cell (Reynolds, 1952).

Fig. 5 summarizes, on a composition *versus* radius-ratio plot, regions where: (i) *I* cells occur and maximizing the number of *M–N* contacts, together with a high value of the packing fraction, generally controls the ordering of the components; (ii) *I* cells occur and maximizing the packing fraction alone controls the ordering; (iii) *P* or *F* cells occur principally to avoid or minimize the number of *M–M* contacts, either because they are large atoms, or for other reasons; (iv) *R* cells occur.

These observations have already led us to predict and find that In_4Ag_9 has a *P* cell rather than *I* as earlier indicated, and that γ-Co–Zn has an *I* cell.

Finally we note that *P* cells have also been reported for three γ-brasses in which one set of the OT sites is 50% or more vacant.

We acknowledge with thanks the support provided for this work by the National Research Council of Canada. We thank Dr C. Calvo of McMaster University, Hamilton, Ontario, who made the Syntex $P\bar{1}$ diffractometer available to us for collection of intensity data for In_4Au_9. We also acknowledge the help provided by Mr V. Fronz in preparing and obtaining single crystals of the alloys and for obtaining powder diffraction photographs of γ-Co–Zn.

References

ALLEN, S. M. & CAHN, J. W. (1972). *Acta Metall.* **20**, 423–433.

BOOTH, M. H., BRANDON, J. K., BRIZARD, R. Y., CHIEH, C. & PEARSON, W. B. (1977). *Acta Cryst.* B**33**, 30–36.

BRADLEY, A. J. & JONES, P. (1933). *J. Inst. Met.* **51**, 131–162.

BRANDON, J. K., BRIZARD, R. Y., CHIEH, P. C., MCMILLAN, R. K. & PEARSON, W. B. (1974). *Acta Cryst.* B**30**, 1412–1417.

BRANDON, J. K., CHIEH, P. C., PEARSON, W. B. & RILEY, P. W. (1975). *Acta Cryst.* A**31**, 236–240.

BRANDON, J. K., PEARSON, W. B., RILEY, P. W., CHIEH, C. & STOKHUYZEN, R. (1977). *Acta Cryst.* B**33**. In the press.

BRIZARD, R. Y. (1975). *Crystal Structure Studies of γ-Brass Phases.* Thesis, Univ. of Waterloo, Waterloo, Ontario, Canada.

EKMAN, W. (1931). *Z. phys. Chem.* B**12**, 57–78.

FRANK, F. C. & KASPER, J. S. (1958). *Acta Cryst.* **11**, 184–190.

FUCHS, K. (1935). *Proc. Roy. Soc.* A**151**, 585–602.

HEIDENSTAM, O. VON, JOHANSSON, A. & WESTMAN, S. (1968). *Acta Chem. Scand.* **22**, 653–661.

HEINE, V. & WEAIRE, D. (1970). *Solid State Physics*, Vol. **24**, pp. 249–463. New York: Academic Press.

HELLNER, E. (1951). *Z. Metallkd.* **42**, 17–19.

HELLNER, E. & LAVES, F. (1947). *Z. Naturforsch.* A**2**, 177–183.

International Tables for X-ray Crystallography (1968). Vol. III, 2nd ed., pp. 201–216. Birmingham: Kynoch Press.

International Tables for X-ray Crystallography (1969). Vol. I, 3rd ed. Birmingham: Kynoch Press.

JOHANSSON, A., LJUNG, H. & WESTMAN, S. (1968). *Acta Chem. Scand.* **22**, 2743–2753.

LAVES, F. (1956). *Theory of Alloy Phases*, pp. 124–198. Cleveland: American Society for Metals.

PARTHÉ, E. (1961). *Z. Kristallogr.* **115**, 52–79.

PAULING, L. (1947). *J. Amer. Chem. Soc.* **69**, 542–553.

PEARSON, W. B. (1958). *A Handbook of Lattice Spacings and Structures of Metals and Alloys.* New York: Pergamon Press.

PEARSON, W. B. (1967). *A Handbook of Lattice Spacings and Structures of Metals and Alloys*, Vol. 2. New York: Pergamon Press.

PUŠELJ, M. & SCHUBERT, K. (1975). *J. Less-Common Met.* **41**, 33–44.

REYNOLDS, J. (1952). Thesis, Oxford Univ.

RICHARDS, M. J. & CAHN, J. W. (1971). *Acta Metall.* **19**, 1263–1278.

SCHRAMM, J. (1938). *Z. Metallkd.* **30**, 10–14, 122–130.

SHOLL, C. A. (1967). *Proc. Phys. Soc.* **92**, 434–445.